Molecular Vision 2016; 22:1375-1386 <http://www.molvis.org/molvis/v22/1375>
Received 5 May 2016 | Accepted 30 November 2016 | Published 2 December 2016

Role of endogenous insulin gene enhancer protein ISL-1 in angiogenesis

Si-qi Xiong, Hai-bo Jiang, Yan-xiu Li, Hai-bo Li, Hui-zhuo Xu, Zhen-kai Wu, Wei Zheng, Xiao-bo Xia

Department of Ophthalmology, Xiangya Hospital, Central South University, Changsha, P.R.China

Objective: To elucidate the role of insulin gene enhancer protein ISL-1 (Islet-1) in angiogenesis and regulation of vascular endothelial growth factor (VEGF) expression in vitro and in vivo.

Methods: siRNA targeting Islet-1 was transfected to human umbilical vein endothelial cell lines (HUVECs). The expression of Islet-1 and VEGF in the cultured cells was measured using real-time PCR and immunoblotting. 3-[4,5-dimethylthiazol-2-yl]-2,5- diphenyltetrazolium bromide; thiazolyl blue (MTT) assay was used to analyze the proliferation of HUVECs affected by Islet-1. Wound healing and Transwell assays were conducted to assess the motility of HUVECs. The formation of capillary-like structures was examined using growth factor–reduced Matrigel. siRNA targeting Islet-1 was intravitreally injected into the murine model of oxygen-induced retinopathy (OIR). Retinal neovascularization was evaluated with angiography using fluorescein-labeled dextran and then quantified histologically. Real-time PCR and immunoblotting were used to determine whether local Islet-1 silencing affected the expression of Islet-1 and VEGF in murine retinas.

Results: The expression of Islet-1 and VEGF in HUVECs was knocked down by siRNA. Reduced endogenous Islet-1 levels in cultured cells greatly inhibited the proliferation, migration, and tube formation in HUVECs in vitro. Retinal neovascularization following injection of Islet-1 siRNA was significantly reduced compared with that of the contralateral control eye. Histological analysis indicated that the neovascular nuclei protruding into the vitreous cavity were decreased. Furthermore, the Islet-1 and VEGF expression levels were downregulated in murine retinas treated with siRNA against Islet-1.

Conclusions: Reducing the expression of endogenous Islet-1 inhibits proliferation, migration, and tube formation in vascular endothelial cells in vitro and suppresses retinal angiogenesis in vivo. Endogenous Islet-1 regulates angiogenesis via VEGF.

Angiogenesis is the formation of new blood vessels from preexisting vasculature. Angiogenesis plays an important role in the pathophysiology of wound healing, ischemic cardiomyopathy, cancer, stroke, atherosclerosis, and ischemic ocular disease. The search for angiogenic factors is largely driven by the need for new treatments for these diseases. The list of putative angiogenic factors is continuously growing. However, vascular endothelial growth factor (VEGF), one of the first angiogenic factors identified, is widely believed to be the most important regulator of healthy and pathological angiogenesis [1]. Therapy targeting VEGF has opened up new vistas for clinical treatment of ocular neovascularization. Anti-VEGF antibodies, such as Avastin [2], Lucentis [3], and Macugen [4], exhibit effective therapeutic potential against retinal and choroidal neovascularization clinically, with minimal toxicity to intraocular tissues. Furthermore, anti-VEGF therapy is particularly promising for the treatment of cancer, by blocking angiogenesis in tumors resistant to conventional therapy [5].

Although VEGF plays a key role in neoangiogenesis and anti-VEGF therapy is clinically attractive for most patients, anti-VEGF interventions are not always satisfactory due to the extremely complex pathophysiology. In addition to VEGF, various cytokines, adhesion molecules, and proteases play an important role [6]. The expression of these angiogenic factors is regulated by upstream transcription factors. Transcription factors determine gene expression by binding to the specific DNA sequences within the promoter regions, forming multiunit complexes with coregulatory proteins, to allow transcriptional activation or repression. Numerous transcription factors, including hypoxia-inducible factor 1α (HIF-1α) [7], nuclear factor kappa B (NF-κβ) [8], E26 transformation-specific-1(Ets-1) [9], c-Jun [10], and PPARgamma-coactivator-1a (PGC-1a) [11], have been found to regulate the expression of angiogenic cytokines and adhesion molecules in neoangiogenesis via different regulatory pathways. Therefore, the increased focus on exploration of novel transcription factors that regulate the expression of

Correspondence to: Xiao-bo Xia,Department of Ophthalmology, Xiangya Hospital, Central South University, Changsha, P.R. China., Phone:+8615874898016; FAX: +867314328960; email: xbxia@yahoo.com

angiogenic factors provides insight into the mechanism of angiogenesis and offers a potential target for gene therapy.

Insulin gene enhancer binding protein-1 (Islet-1) is a LIM domain transcription factor belonging to the LIM homeodomain subfamily [12]. As a key transcription factor, Islet-1 regulates cell fate and embryonic development [13]. Islet-1 also plays an important role in cell specification, differentiation, and maintenance of phenotypes of the ganglion, cholinergic amacrine, ON bipolar, and horizontal cells in the retina [14]. Recently, it has been demonstrated that gene transfer of Islet-1 into cultured vascular endothelial cells improves proliferative, migratory, and tube formation properties, which are attributed to increased secretion of VEGF [15]. Conditioned medium from human mesenchymal stem cells overexpressing Islet-1 dramatically improves survival, migration, and tube formation in human umbilical vein endothelial cells (HUVECs) in vitro and in vivo. The monocyte chemoattractant protein-3 (MCP3) was found to be concomitantly upregulated after forced expression of Islet-1 in human mesenchymal stem cells [16]. Furthermore, in an experimental infarction model, delivery of Islet-1 into areas of myocardial infarction improved the therapeutic outcome by promoting angiogenesis [17]. These results indicate that overexpression of Islet-1 in cells by gene transfer promoted angiogenesis. However, the role of endogenous Islet-1 in angiogenesis remains unknown. The role of Islet-1 together with HIF-1α, NF–κβ, Ets-1, and PGC-1a in regulating neoangiogenesis has yet to be determined. Therefore, using cultured HUVECs, we analyzed whether inhibition of endogenous Islet-1 altered their proliferation, migration, and tube formation in vitro and examined whether suppression of Islet-1 in the retinas of murine models of oxygen-induced retinopathy (OIR) inhibited pathological retinal neovascularization in vivo.

METHODS

Materials: The study protocol conformed to the ARVO Statement for the Use of Animals in Ophthalmic and Vision Research and approved by the Ethics Review Committees for Animal Experimentation of Central South University. Small interference RNA (GIMA siRNA company, Shanghai, China). anti-Islet-1 antibody (Abcam , Cambridge, England),rabbit polyclonal anti-VEGF antibody (Abcam), Transwell (Corning Costar, Corning, NY), Matrigel (BD Biosciences, San Jose, CA), C57BL/6J mice (Shanghai Laboratory Animal Center, Shanghai,China).

siRNA synthesis: siRNA targeting human Islet-1 mRNA (siRNA1) and murine Islet-1 mRNA were designed. The sense strand of siRNA1 against human Islet-1 was 5′- . The sense strand was 5′-AAA AGA AUG GAG GUG GAA GdT dT-3′, and the antisense strand was 3′- dTd TUU UUC UUA CCU CCA CCU UC-5′. The sense strand of siRNA targeting murine Islet-1 mRNA was 5′-UCA GCU UCA UAU AGA CAA AdT dT-3′, and the antisense strand was 3′-dTd TAG UCG AAG UAU AUC UGU UU-5′. One negative control siRNA that has homology limited to sequences in the human and mouse genomes and three Islet-1 siRNA were synthesized and purified by the GIMA siRNA company (Shanghai, China).

Cell culture and transfection: HUVECs were purchased from the American Type Culture Collection (Manassas, VA). The HUVECs were grown in F12K medium, containing 0.1 mg/ml heparin, 20% fetal bovine serum, and 0.03 mg/ml endothelial cell growth supplement. The cells were cultured in an incubator at 37 °C in an atmosphere of 95% air and 5% CO_2. Transfection reagent Lipofectamine 2000 (Invitrogen, Carlsbad, CA) [18]. was used to transfer the siRNA targeting Islet-1 into the HUVECs according to the manufacturer's protocol.

Real-time PCR: Total RNA was isolated from cultured cells or retinal tissues with TRIzol® reagent (Invitrogen).The first strand cDNA was synthesized using an oligo (dt) primer in the First Strand cDNA Synthesis kit (Fermentas, Hanover, MD). The specific primers for human and murine Islet-1, VEGF and β-actin, were designed and synthesized by Bio Basic Inc. (Shanghai, China). To amplify human Islet-1 in cultured cells, the primer pair, 5′-AGA TCA GCC TGC CTG CTT TTC AGC-3′ (sense) and 5′-AGG ACT GGC TAC CAT GCT GT-3′ (antisense), was used to generate the Islet-1 PCR product. The primer pair, 5′-TCT CCC TGA TCG GTG ACA GT-3′ (sense) and 5′-CAC ACA AAT ACA AGT TGC CA-3′ (antisense), was used to yield the PCR product of human VEGF. The primer pair, 5′-GTC CAC CTT CCA GCA GAT GT-3′ (sense) and 5′-AAA GCC ATG CCA ATC TCA TC-3′ (antisense), was designed to generate the PCR product of human β-actin. To amplify Islet-1 in the murine retinas, the primer pair, 5′-CGG ATC CTA CAG ATA TGG GA-3′ (sense) and 5′-CGT CGA CTC CTC ATG CC CTC-3′ (antisense), was used to generate the PCR product. The primer pair, 5′-TAT TTG GCA ACT TGT GTT TG-3′ (sense) and 5′-GAA TTC TCT ATT TTT CTT GT-3′(antisense), was used to yield the PCR product of murine VEGF. The primer pair, 5′-TGG TTA CAG GAA GTC CC TCA-3′ (sense) and 5′-AAG CAA TGC TGT CAC CTT CC-3′ (antisense), was designed to generate the PCR product of murine β-actin. The program cycle was set as follows: thermal profile consist of 10 min of annealing at 50 °C, one cycle at 95 °C and 5 min of polymerase activation followed by 45 cycles of PCR for 10 s at 95 °C and 59 °C for 30 s followed by melt curve analysis performed at

65–95 °C with increment of 0.5 °C for 10 s to confirm the authenticity of the amplified product by its specific melting temperature (Tm). The quantity of mRNA was calculated based on the cycle threshold (CT) values that were standardized with the amount of the housekeeping gene β-actin. An additional calculation was performed using the $2^{-\Delta\Delta CT}$ method, and the results were expressed as an n-fold difference relative to normal controls.

Western blot analysis: The cultured cells and the entire murine retinas were collected and lysed in lysis buffer containing protease inhibitors (Boehringer, Mannheim, Germany). Total protein (30 µg per lane) was resolved on sodium dodecyl sulfate–polyacrylamide gel and transferred on a nitrocellulose membrane and incubated with rabbit polyclonal anti-Islet-1 antibody (Abcam, 1:1,000), rabbit polyclonal anti-VEGF antibody (Abcam, 1:1,000) and mouse monoclonal anti-β-actin antibody (Sigma, St. Louis, MO, 1:5,000), followed by incubation with corresponding secondary antibodies: goat anti-rabbit antibody (Abcam, 1:3,000) or goat anti-mouse antibody (Abcam, 1:2,000). The enhanced chemiluminescence (ECL) reagent was added to the membrane as instructed by the manufacturer. Briefly, the substrate working solution was prepared by mixing equal parts of the detection reagents. About 0.125 ml working solution per cm^2 of membrane was used. The blot was incubated with working solution for 1 min at room temperature. The membrane was exposed to an X-ray film for 1 min before it was developed and fixed.

MTT assay: 3-[4,5-dimethylthiazol-2-yl]-2,5- diphenyltetrazolium bromide; thiazolyl blue (MTT) was used to measure the proliferation of HUVECs. A total of 1×10^4 HUVECs were inoculated in 96-well flat-bottomed plates. After treatment with Islet-1-siRNA or negative control siRNA, the cells were cultured for 6 days. Every 24 h, the MTT solution (5 mg/ml) was added to a group of wells. Following 4 h incubation at 37 °C, the cell culture medium was removed, and 100 µl of dimethyl sulfoxide (DMSO) was added to solubilize the crystals. The absorbance of each well was measured with an ELx800 Universal Microplate Reader (Bio-Tek, Winooski, VT) with the detection wavelength set at 570 nm. The relative proliferation level of cells was measured as the optical density (OD) value [19].

Invasion and migration assay: For the invasion assay, the Transwell with an 8 µm diameter pore membrane (Costar, Corning, NY) was coated with 200 µl Matrigel at 200 µg/ml and incubated overnight. Twenty-thousand HUVECs with or without transfection of siRNA targeting Islet-1 were seeded into the upper chamber of the Transwell. After 24 h of incubation at 37 °C, the cells were fixed in methanol and stained with hematoxylin and eosin (H&E), and the cells that invaded through the pores to the lower surface of the filter were counted under a microscope. Three invasion chambers were used per condition. The values obtained were calculated by averaging the total number of cells from three filters. For the migration assay, a wound-healing assay was performed. HUVECs (1×10^6) were seeded on 6 cm plates coated with 10 µg/ml type I collagen. The cells were incubated for 24 h, and then the monolayer was disrupted with a cell scraper. The cells were incubated in a medium without fetal bovine serum, and photographs were taken at 0 and 48 h in a phase-contrast microscope (Nikon ELWD 0.3 ,Tokyo, Japan). The distance of the wounded region lacking cells was measured, and the results were displayed as the wound healing rate. Experiments were performed in triplicate, and four fields of each point were recorded.

In vitro tube formation assay: In vitro formation of capillary-like structures was examined using growth factor reduced Matrigel (BD Biosciences, San Jose, CA). Cell suspensions containing 50 ng/ml VEGF were plated on Matrigel-coated 48-well plates at a density of 25,000 cells per well in endothelial basal medium (EBM) containing 0.2% fetal calf serum (FCS). Cells were directly photographed after 18 h with a Leica camera (Leica, Wetzlar, Germany; 40× magnification). The photographs were analyzed using Image J software, and network structures and capillary-like areas were separately marked. We measured the relative capillary-like structure density by computing the number of capillary-like areas, and took the normal group as 100%. The experiments were repeated at least three times.

Animal model of proliferative retinopathy: The study protocol conformed to the ARVO Statement for the Use of Animals in Ophthalmic and Vision Research. The reproducible mouse model of oxygen-induced retinopathy (OIR) has been described previously [20]. At postnatal day 7 (P7), the C57BL/6J mice were exposed to 75% ± 2% oxygen for 5 days with the nursing mothers. The mice were removed from the chamber at P12 and maintained in room air until P17. Mice of the same strain and of the same age were kept in room air and used as control subjects. Intravitreal injections were performed at P12.

Intravitreal injections: At P12, the mice were anaesthetized with an intraperitoneal (IP) injection of pentobarbital sodium. The lid fissure was opened using a no. 11 scalpel blade, and the eye was proptosed. Intravitreal injections were performed by first entering the eye with an Ethicon TG140–8 suture needle at the posterior limbus. A 32-gauge Hamilton needle and syringe were used to deliver 1 µl liposome-Islet-1 siRNA

(5 µg) complex or 1 µl control complex (liposome-negative control siRNA) into the vitreous cavity.

Angiography with high-molecular-weight fluorescein-dextran: At P17, mice were anesthetized with a 30 mg/kg intraperitoneal injection of sodium pentobarbital sodium, and perfused through the left ventricle with PBS (NaCl 8.00 g, KCl 0.20 g ,Na_2HPO_4 1.44 g, 0.24 g KH_2PO_4 , pH 7.4) 1 ml of 50 mg/ml fluorescein labeled high molecular weight (2,000,000) dextran (Sigma-Aldrich). Subsequently, the mice were sacrificed and the eyes were enucleated. The retinas were dissected and flatmounted on microscope slides with glycerol-gelatin. Adobe Photoshop CS3 (Adobe Photoshop CS3; Adobe Systems, Inc., San Jose, CA) was used for the quantification of vaso-obliteration, which was processed as described previously [21].

Histological analysis of neovascularization: The P17 mice were killed with IP injections of an overdose of sodium pentobarbital. Their eyes were enucleated, fixed with 4% paraformaldehyde in PBS, and embedded in paraffin. Serial 6 µm paraffin-embedded axial sections of the retina were obtained starting at the optic nerve head. After staining with periodic acid-Schiff reagent and hematoxylin, ten intact sections of equal length, each 30 µm apart, were evaluated for a span of 300 µm. All retinal vascular cell nuclei anterior to the internal limiting membrane were counted in each section according to a fully masked protocol. Averaging of all ten counted sections yielded the mean number of neovascular cell nuclei per 6 µm section per eye.

Immunohistochemistry: Retinal sections were obtained from mouse eyes fixed in 4% paraformaldehyde in PBS for 1 h on ice. The eyes were embedded in optimal cutting temperature (OCT) medium (Sakura Finetechnical, Torrance, CA) and snap frozen in liquid nitrogen. Frozen retinal sections were cut in a cryostat at 10 µm thickness along the vertical median through the optic nerve. Sections were rehydrated in PBS and blocked with blocking buffer (10% ChemiBlocker; Millipore, Billerica, MA) in PBS for 30 min at room temperature. Primary antibody rabbit polyclonal anti-Islet-1 antibody (Abcam, 1:250) was incubated in PBS containing 0.05% Tween 20 (PBTS) buffer overnight at 4 °C. The sections were washed with PBTS buffer five times (5 min each at room temperature). The slides were incubated with Alexa Fluor 488 anti-rabbit (Jackson ImmunoResearch, West Grove, PA; 1:200) 1 h at room temperature. The sections were washed with PBTS buffer five times (5 min each at room temperature) and rinsed with PBS. The chromosomal DNA was stained with 4', 6-diamidino-2-phenylindole (DAPI; Roche diagnostics) and covered with a glass coverslip. Confocal fluorescence microscopy was performed using a Leica SP2. Images were subsequently processed using IMARIS (Bitplane Inc., Zurich, Switzerland) and Adobe Photoshop CS4 (Adobe Systems Inc).

Statistical analysis: The results were expressed as mean ± standard error of the mean (SEM). One-way ANOVA followed by the least significant differences (LSD) *t* test were used to evaluate significant differences. A p value of less than 0.05 was considered statistically significant.

RESULTS

Decreased expression of Islet-1 correlates with VEGF expression in HUVECs: To correlate Islet-1 expression with VEGF mRNA transcription, we used the siRNA approach to silence the expression of Islet-1. We designed an Islet-1 siRNA sequence to inhibit the expression of Islet-1 in HUVECs. Real-time PCR and western blotting were conducted to assess the inhibition of gene transcription and translation. As shown in Figure 1, siRNA inhibited the protein expression of Islet-1 by >80%, as well as its mRNA transcription (Figure 1 A,B). As expected, VEGF expression was also downregulated by >50% ($p<0.05$; Figure 1C,D).

Knockdown of Islet-1 inhibits proliferation of HUVECs: The MTT assay was performed to analyze the proliferation of HUVECs affected by Islet-1. The cells were treated with Islet-1-siRNA or negative control siRNA. Every 24 h, the absorbance of samples was read and recorded as the OD value. The quantity of MTT crystallization is proportional to the number of surviving cells, and the OD value can indirectly reflect the number of surviving cells. Compared with the negative control group, Islet-1 siRNA inhibited the proliferation rate of HUVECs by 41.9% on day 6 ($p<0.05$; Figure 2A).

Downregulation of Islet-1 inhibited HUVECs tube formation in vitro: A key aspect of angiogenesis is the formation of capillary-like tubes by endothelial cells. We tested whether siRNA-mediated downregulation of Islet-1 affected HUVECs tube formation in vitro. Under normal culture conditions, HUVECs gradually stretch and connect each other into network structure, forming luminal structures of various sizes and shapes. The pictures were analyzed using Image J software, and the network structures and capillary-like areas were separately marked. We measured the relative capillary-like structure density by computing the number of capillary-like areas, and took the normal group as 100%. After transfection with siRNA, as shown in Figure 2, the number of tubes in the HUVECs following RNAi was significantly lower than that of the negative control group ($p<0.05$) and the normal control group ($p<0.05$; Figure 2B,C).

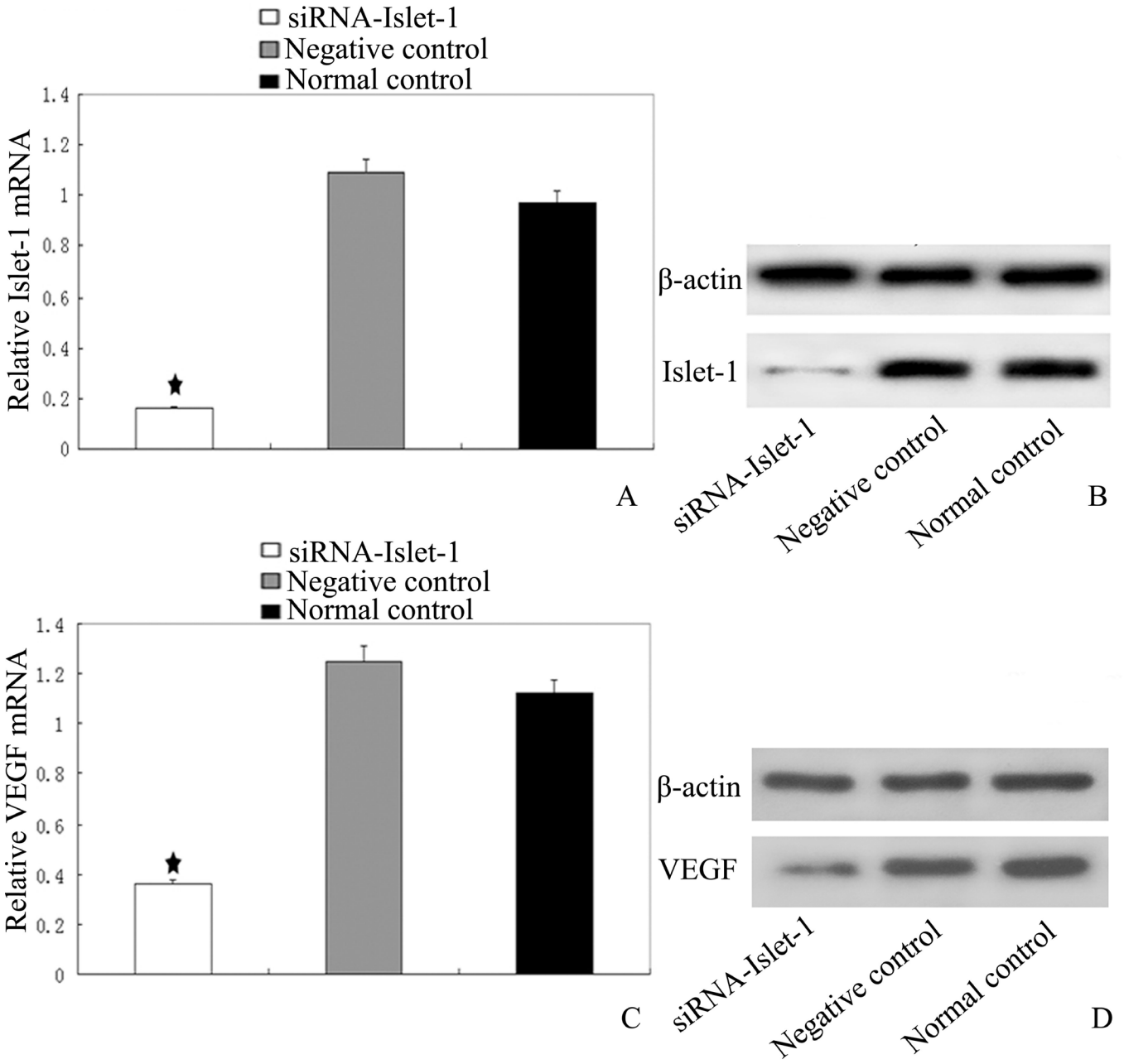

Figure 1. Decreased expression of Islet-1 correlates with VEGF by siRNA targeting Islet-1 in HUVECs. Real-time PCR and western blot analysis were performed to assess inhibition efficiency at the transcription and translation levels. **A**, **B**: Expression of insulin gene enhancer protein ISL-1 (Islet-1) in human umbilical vein endothelial cell lines (HUVECs). siRNA targeting Islet-1 inhibited the protein expression of Islet-1 by >80%, as well as its mRNA transcription. **C**, **D**: Expression of vascular endothelial growth factor (VEGF) in HUVECs at the mRNA and protein levels was also downregulated by >50%, star indicates that the expression of Islet-1 and VEGF mRNA was decreased significantly compared to the controls (star $p<0.05$).

Islet-1 affects invasion and migration of HUVECs in vitro: The in vitro motility was assessed using wound healing and Transwell assays of the HUVECs. The wound healing assay was used to determine the migration of HUVECs. The siRNA-Islet-1 group of cells exhibited a 36% decrease in closure compared with the negative control group ($p<0.05$), suggesting a role for Islet-1 in the migration of HUVECs (Figure 3A,B). To substantiate this observation, a Matrigel invasion assay in Transwell culture chambers was performed to determine the effect of Islet-1 on in vitro invasion of

HUVECs. The number of siRNA-Islet-1 group cells that passed through Matrigel was only 41% compared with the negative control group ($p<0.05$; Figure 3C,D). Together, these results support a critical role for Islet-1 in the motility of HUVECs.

Angiographic evaluation of the role of Islet-1 siRNA in retinal neovascularization: To evaluate the angiostatic efficacy of Islet-1 siRNA on hyperoxia-induced retinal neovascularization, the retinas were examined with fluorescein-dextran perfusion and flat mounting at P17. The retinas of the mice exposed to room atmosphere revealed superficial and deep vascular layers that extended from the optic nerve to the periphery, without neovascular tufts (Figure 4A). However, the retinas from the hyperoxia-exposed mice with a negative control siRNA injection or without an injection contained multiple neovascular tufts and a central non-perfusion area (Figure 4B,C). In contrast, fewer neovascular complexes and a non-perfusion area were found in the retinas of the eyes injected with Islet-1 siRNA (Figure 4D).

Histological analysis of retinal neovascularization: Neovascularization was assessed histologically by counting the endothelial cell nuclei anterior to the inner limiting membrane.

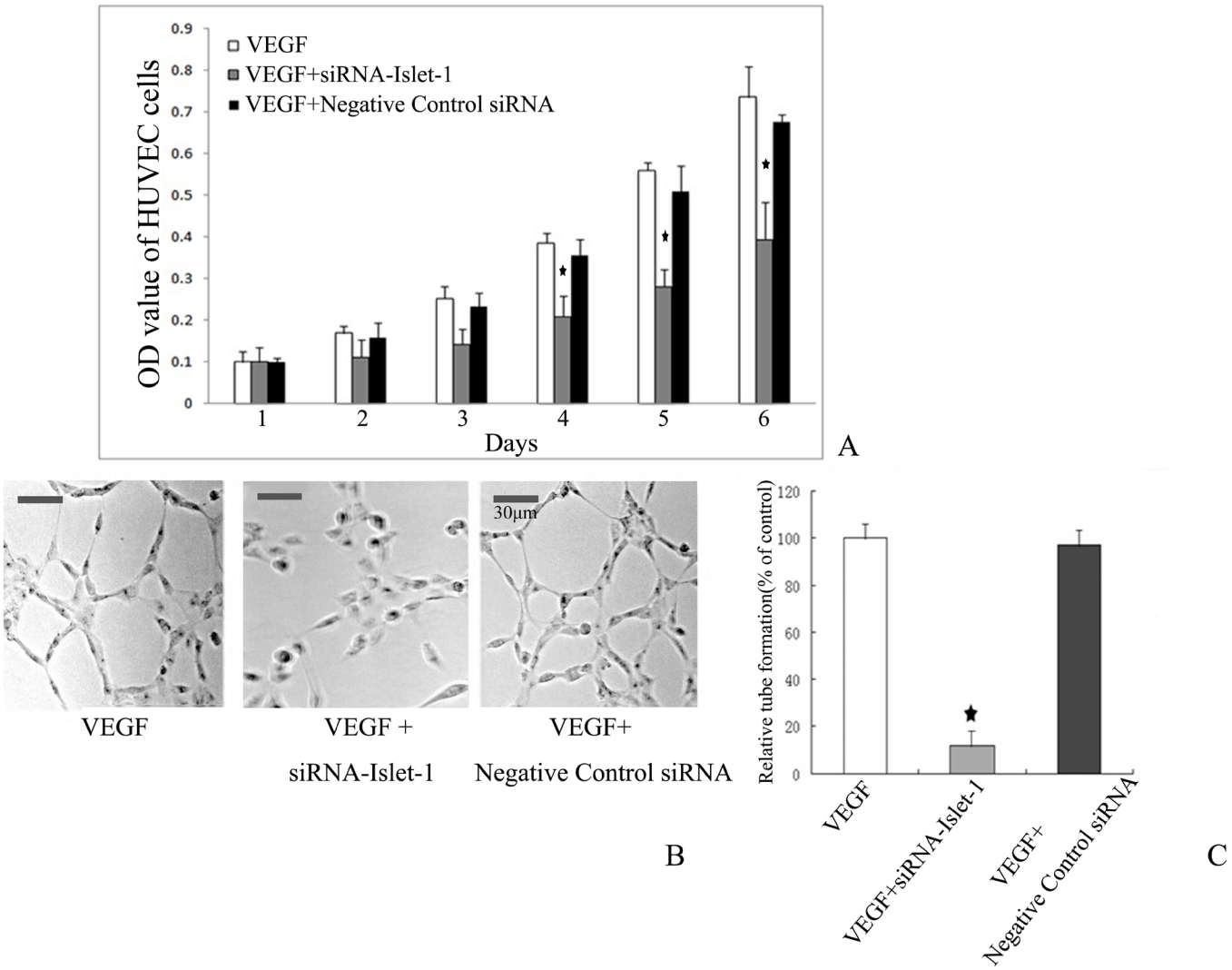

Figure 2. Knockdown of Islet-1 inhibits proliferation and tube formation of HUVECs. **A**: 3-[4,5-dimethylthiazol-2-yl]-2,5- diphenyltetrazolium bromide; thiazolyl blue (MTT) assay was performed to analyze the proliferation ability of human umbilical vein endothelial cell lines (HUVECs) affected by attenuation of cellular Islet-1. Compared to negative control, insulin gene enhancer protein ISL-1 (Islet-1) siRNA inhibited the proliferation rate of HUVECs (star $p<0.05$). **B**, **C**: Downregulation of Islet-1 inhibited the tube formation in HUVECs in vitro. After transfection with siRNA targeting Islet-1, the number of tubes in HUVECs following RNAi was significantly lower than that of the negative control group (star $p<0.05$).

This assessment revealed that the retinas of the un-injected eyes from the hypoxic mice contained multiple neovascular tufts extending into the vitreous (Figure 5B). The amount of preretinal neovascularization in the untreated hypoxic eyes was similar to that of the negative control siRNA-injected eyes (Figure 5C). Intravitreal injections of siRNA targeting Islet-1 in the hypoxic mice reduced the histologically evident retinal neovascularization (Figure 5D) compared with that evident in the negative control siRNA injected or untreated eyes ($p<0.05$). Administration of siRNA against Islet-1 resulted in inhibition of retinal neovascularization, with an inhibitory effect of 50%.

Suppression of Islet-1 and VEGF expression in mouse retinas by siRNA: Five days after intravitreal injection, the mouse retinas were extracted and assessed with real-time PCR and western blotting to assess the expression of Islet-1 and VEGF. In the retinas of hypoxic animals exposed to Islet-1 siRNA, Islet-1 was downregulated (Figure 6A; $p<0.05$). Compared with the control groups, the VEGF levels were also inhibited (Figure 6C; $p<0.05$). Our results showed that the transfection of Islet-1 siRNA into murine retinas resulted in significant silencing of Islet-1 and VEGF expression, resulting in inhibition of retinal neovascularization in an OIR model.

Immunohistochemistry analysis of Islet-1 expression in murine retinas: Positive immunostaining for Islet-1 was detected in the room air–raised mice, which was mainly identified in the inner nuclear and ganglion cell layers (Figure 7A). In contrast, the hyperoxia-exposed mice manifested more intensive immunostaining signal (Figure 7B,C). Administration of siRNA targeting Islet-1 significantly reduced the immunostaining of Islet-1 in the hyperoxia-exposed mouse retina (Figure 7D).

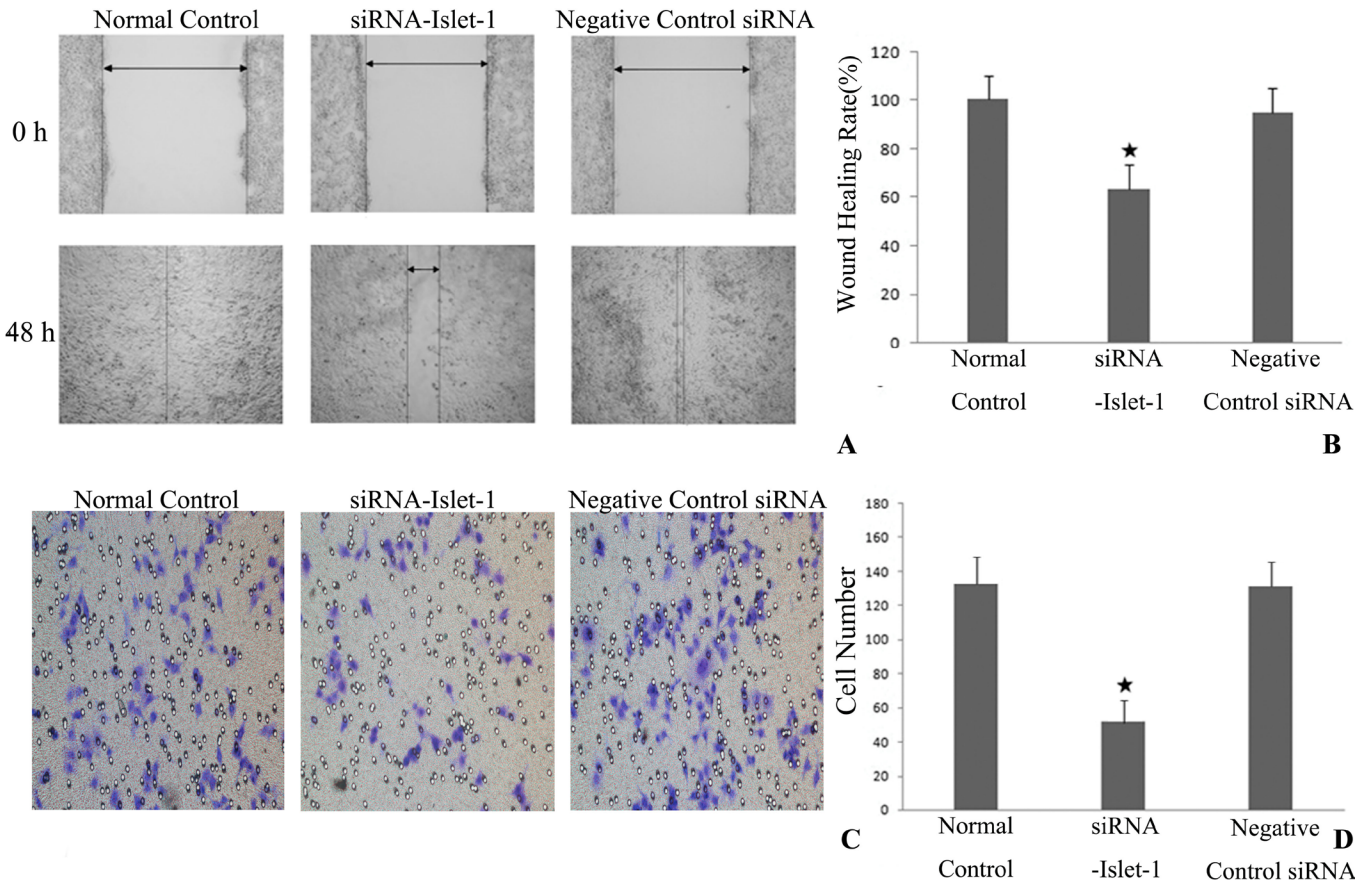

Figure 3. Islet-1 affects the invasion and migration of HUVECs in vitro. For assessment of the migration ability of human umbilical vein endothelial cell lines (HUVECs), the wound healing and Transwell assays were used. **A**, **B**: The siRNA-insulin gene enhancer protein ISL-1 (Islet-1) group cells exhibited a 36% decrease in closure compared with the negative control group (star $p<0.05$), suggesting a role for Islet-1 in the migration of HUVECs. **C**, **D**: A Matrigel invasion assay in the Transwell culture chambers was performed to determine the effect of Islet-1 on the in vitro invasion of HUVECs. The number of siRNA-Islet-1 group cells that passed through Matrigel was only 41% compared with the negative control group (star $p<0.05$). Together, these results support a critical role for Islet-1 in the motility of HUVECs.

DISCUSSION

Islet-1 plays an important role in the development and formation of various organs and tissues [13,22]. The expression of Islet-1 is closely related to the occurrence and progression of various tumors. Islet-1 expression is upregulated in different solid tumors, such as bile duct carcinoma [23], gastrointestinal, pancreatic and lung tumors [24], breast cancer [25], and pheochromocytoma [26]. These studies showed the relationship between Islet-1 and tumorigenesis and development. However, the role of Islet-1 in tumor initiation and progression is still unclear. Tumor growth is closely related to angiogenesis prompting us to speculate whether the expression of transcription factor Islet-1 in tumor tissue is associated with tumor angiogenesis. Islet-1 has been found to promote angiogenesis [15]. Enhanced proliferation was found in capillary endothelial cells that overexpress Islet-1. However, previous studies investigating Islet-1 and angiogenesis mainly focused on the overexpression of exogenous Islet-1 in cells to increase angiogenesis. Until now, the relationship between endogenous Islet-1 and angiogenesis under pathophysiological conditions has never been reported. Murine models of OIR represent a major tool for the investigation of pathological angiogenesis associated with ischemia. As the neovascular response is consistent, reproducible, and quantifiable, it was commonly used to study molecules that participate in retinal angiogenesis and related antiangiogenic treatments [20]. In this study, we found that inhibition of Islet-1 expression in retinal tissue reduced retinal neovascularization in murine models of OIR. After delivery of siRNA targeting Islet-1 into the vitreous cavity, we found that the neovascular endothelial cells permeating the inner limiting membrane of the retina were reduced. Leakage of new blood vessels was inhibited, and the retinal non-perfusion area was decreased, indicating that the suppression of endogenous Islet-1 inhibited pathological retinal angiogenesis.

To elucidate the underlying mechanism, we cultured vascular endothelial cells in vitro. We found that the expression of Islet-1 in vascular endothelial cells was inhibited by siRNA targeting Islet-1. Furthermore, Islet-1 inhibition significantly downregulated the expression of endogenous

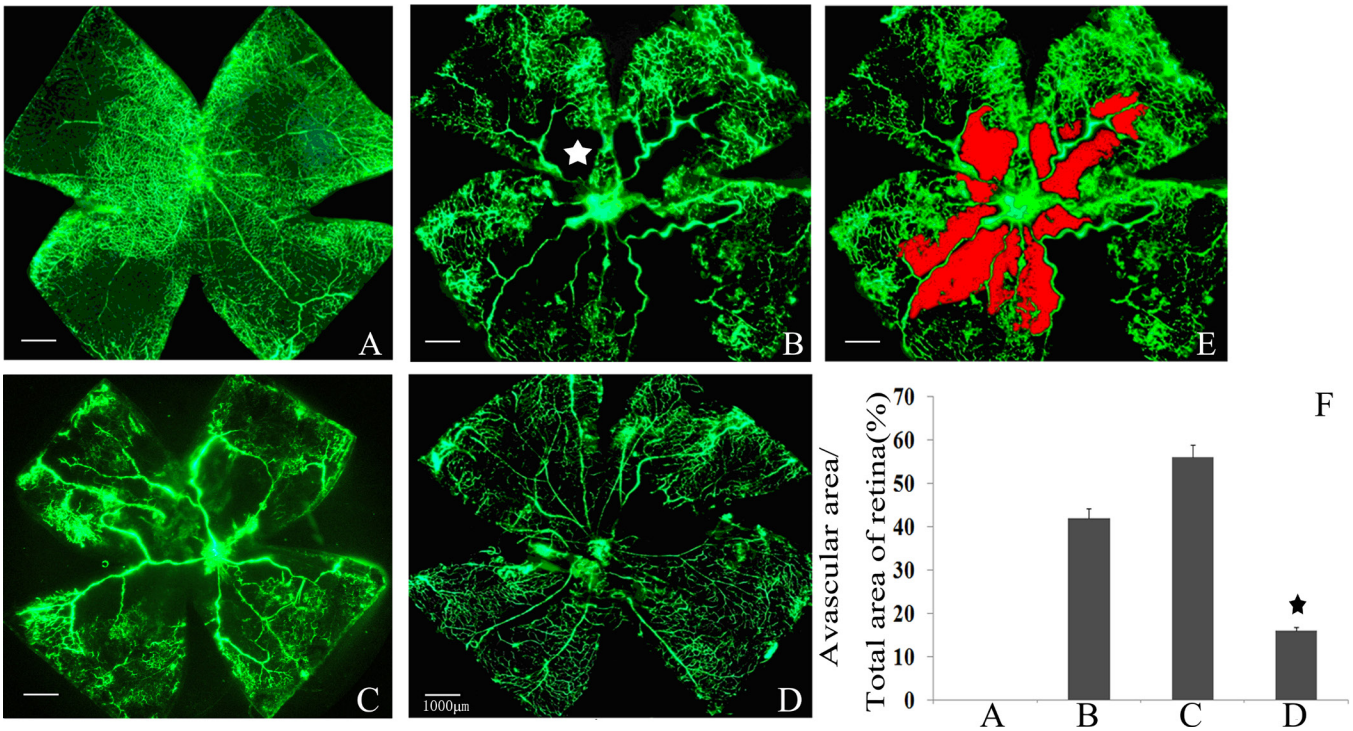

Figure 4. Angiographic analysis of the effect of Islet-1 siRNA on retinal neovascularization in the mouse. **A**: Room air–raised mice with normal retinal vessel structure. **B**: In the murine model of oxygen-induced retinopathy (OIR), neovascular tufts (indicated by the arrow) appear as hyperfluorescence at the junction between the perfused and non-perfused areas (indicated with a star). **C**: The murine OIR model with injection of negative control siRNA. Neovascular tufts are apparent at the junction between the perfused and non-perfused areas. **D**: The murine OIR model injected with siRNA targeting insulin gene enhancer protein ISL-1 (Islet-1). **E**: The red area indicates the non-perfusion area. **F**: The non-perfusion areas were reduced after intravitreal injection of siRNA against Islet-1 compared with that of the murine model of OIR (star $p<0.05$).

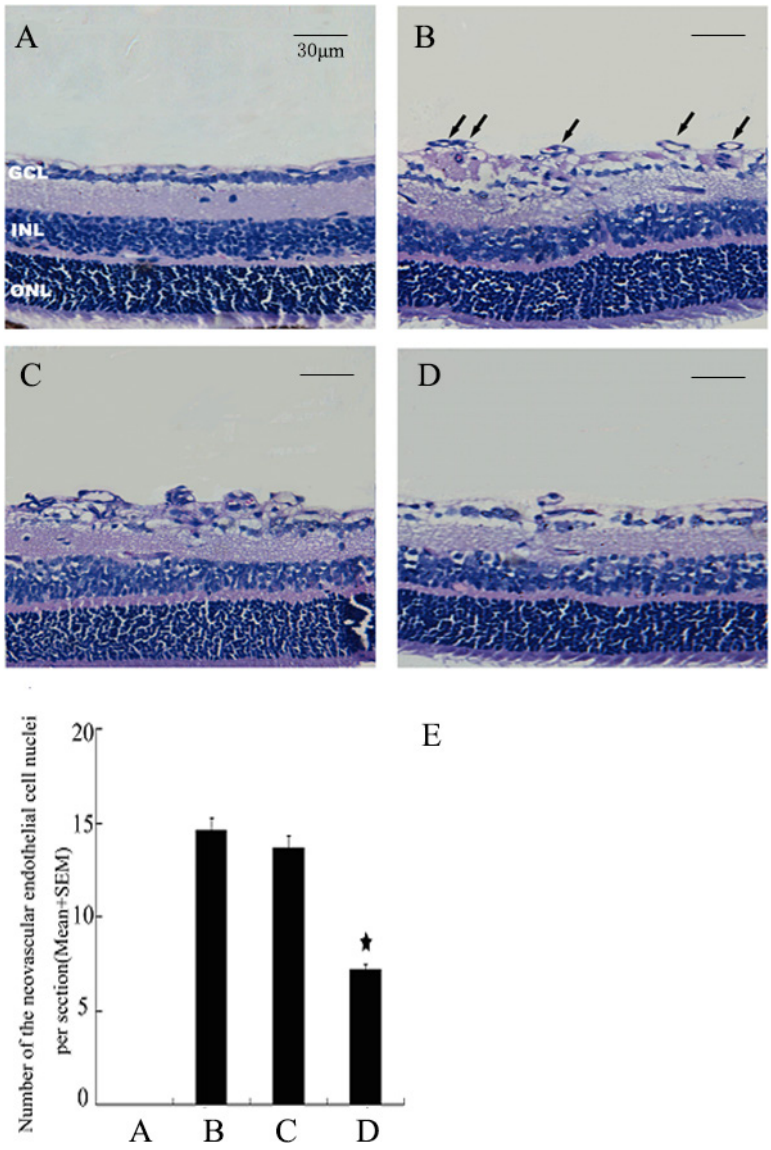

Figure 5. Histological analysis of inhibition of ischemia-induced retinal neovascularization by siRNA targeting Islet-1. **A**: Room air–raised mice. **B**: The murine model of oxygen-induced retinopathy (OIR). **C**: The murine OIR model with injection of negative control siRNA. **D**: The murine OIR model injected with siRNA targeting insulin gene enhancer protein ISL-1 (Islet-1). **E**: Retinal neovascularization was assessed histologically by counting the endothelial cell nuclei protruding into the vitreous cavity. The mean number of neovascular cell nuclei in eyes injected with Islet-1 siRNA was approximately 50% of the number in the eyes of the murine model of OIR (star $p<0.05$). GCL = ganglion cell layer; INL = inner nuclear layer; ONL= outer nuclear layer.

VEGF, and decreased the migration, proliferation, and tube formation of the vascular endothelial cells. Injection of the siRNA Islet-1 into the vitreous cavity significantly decreased the expression of Islet-1 in the retina compared with the murine model of OIR. We surmised that intravitreal siRNA targeting Islet-1 penetrates the internal limiting membrane into the retinal cells, to bind with the RNA-induced silencing complex (RISC). The activated RISC splices the Islet-1 mRNA at the site of the homologous sequence in retinal cells [27]. The activated RISC binds and destroys hundreds of Islet-1 mRNAs in retinal tissues. Downregulation of Islet-1 in murine retinal cells may reduce VEGF, to suppress retinal angiogenesis in the murine model of OIR by inhibiting the proliferation, migration, and tube formation of retinal vascular endothelial cells. Recent studies suggest that Islet-1 promotes angiogenesis by increasing the expression of monocyte chemoattractant protein-3 [16]. We speculated that the VEGF and chemoattractant protein-3 levels, together with

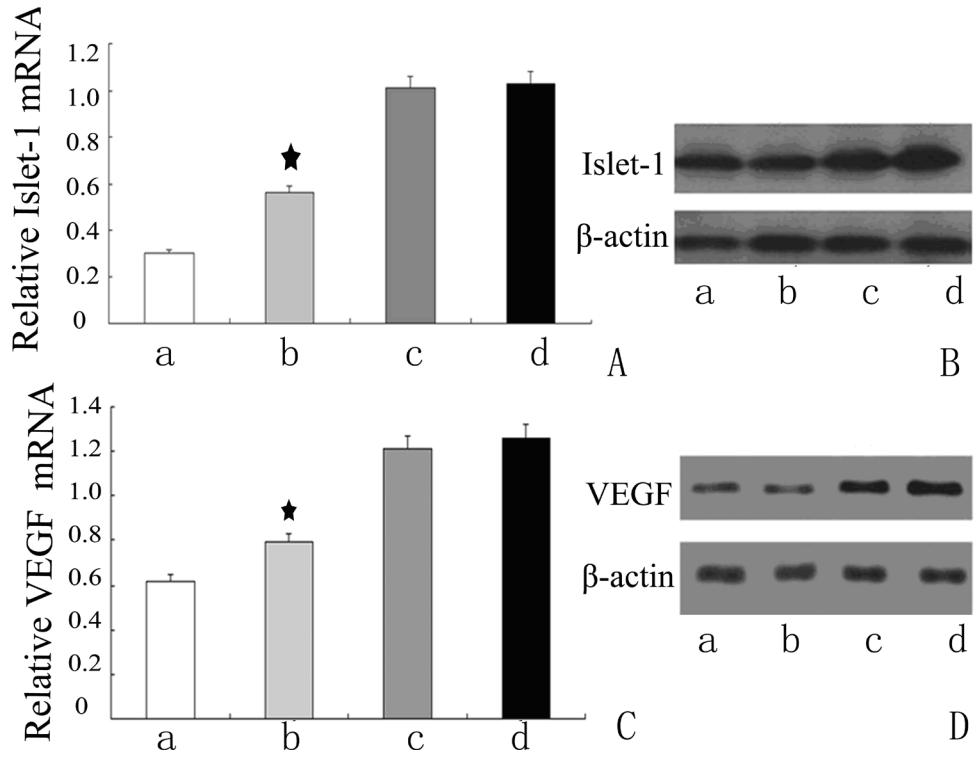

Figure 6. Inhibition of Islet-1 and VEGF expression in murine retinas by siRNA targeting Islet-1. Real-time PCR and western blot analysis for Islet-1 and the vascular endothelial growth factor (VEGF) level in murine retinas. The level of Islet-1 and VEGF in the murine retinas was decreased after local administration of Islet-1 siRNA compared to the model of oxygen-induced retinopathy (OIR) (star $p<0.05$). **A**: Room air–raised mice. **B**: The murine OIR model injected with siRNA targeting Islet-1. **C**: The murine OIR model with injection of negative control siRNA. **D**: The murine model of OIR.

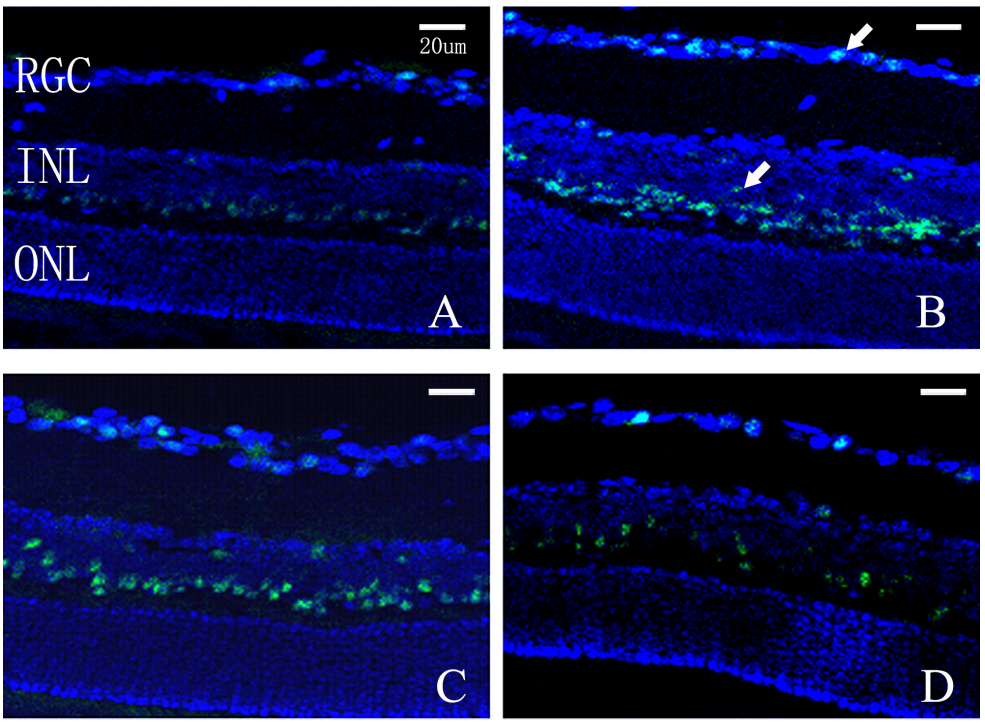

Figure 7. Immunohistochemistry analysis of Islet-1 expression in murine retinas. **A**: Room air–raised mice. **B**: The murine model of oxygen-induced retinopathy (OIR). **C**: The murine OIR model with injection of negative control siRNA. **D**: The murine OIR model injected with siRNA targeting Islet-1. Positive immunostaining for Islet-1 was detected at the inner nuclear and ganglion cell layers in the room air–raised mice. A more apparent immunostaining signal was found in the murine model of OIR. SiRNA against Islet-1 decreased the immunostaining of Islet-1 in the hyperoxia-exposed mouse retina. RGC = retinal ganglion cell; INL = inner nuclear layer; ONL = outer nuclear layer.

other unknown angiogenic factors regulated by Islet-1, may be reduced by siRNA targeting Islet-1. Inhibition of these angiogenic factors by siRNA targeting Islet-1 resulted in suppression of retinal angiogenesis.

In summary, our results show that inhibition of endogenous Islet-1 expression inhibits the proliferation, migration, and tube formation of vascular endothelial cells in vitro, and retinal angiogenesis was suppressed by downregulating the expression of Islet-1 in vivo. The role of endogenous Islet-1 in regulating angiogenesis is related to VEGF. Therefore, this study indicated that Islet-1 may take part in the process of angiogenesis accompanied by VEGF, which further clarified the molecular mechanism of angiogenesis.

ACKNOWLEDGMENTS

This research was supported by National Natural Science Foundation of China (Grant No.81000388) , Health and Family Planning Commission of Hunan Province (Grant No.132015016) and Natural Science Foundation of Hunan Province(Grant No.12JJ3120). The authors declare no competing financial interests. Si-qi Xiong designed the research, interpreted the data and wrote the paper, Wei Zheng , Hai-bo Jiang ,Yan-xiu Li , Zhen-kai Wu and Hai-bo Li contributed to acquisition of data, Hai-bo Jiang and Hui-zhuo Xu contributed to analysis and interpretation of data, Xiao-bo Xia proofread the manuscript. All authors showed final approval of the version to be submitted. Xiao-bo Xia (xbxia@yahoo.com) and Wei Zheng (zhengweiinxy@126.com) contributed equally to this work.

REFERENCES

1. Pe'er J, Shweiki D, Itin A, Hemo I, Gnessin H, Keshet E. Hypoxia-induced expression of vascular endothelial growth factor by retinal cells is a common factor in neovascularizing ocular diseases. Lab Invest 1995; 72:638-45. [PMID: 7540233].
2. Avery RL, Pearlman J, Pieramici DJ, Rabena MD, Castellarin AA, Nasir MA, Giust MJ, Wendel R, Patel A. Intravitreal bevacizumab (Avastin) in the treatment of proliferative diabetic retinopathy. Ophthalmology 2006; 113:1695- [PMID: 17011951].
3. Rothenbuehler SP, Waeber D, Brinkmann CK, Wolf S, Wolf-Schnurrbusch UE. Effects of ranibizumab in patients with subfoveal choroidal neovascularization attributable to age-related macular degeneration. Am J Ophthalmol 2009; 147:831-7. [PMID: 19217019].
4. González VH. [1], Giuliari GP, Banda RM, Guel DA. Intravitreal injection of pegaptanib sodium for proliferative diabetic retinopathy. Br J Ophthalmol 2009; 93:1474-8. [PMID: 19692371].
5. Selle F, Emile G, Pautier P, Asmane I, Soares DG, Khalil A. Alexandre J, Lhommé C, Ray-Coquard I, Lotz JP, Goldwasser F, Tazi Y, Heudel P, Pujade-Lauraine E, Gouy S, Tredan O, Barbaza MO, Ady-Vago N, Dubot C. Safety of bevacizumab in clinical practice for recurrent ovarian cancer: A retrospective cohort study. Oncol Lett 2016; 11:1859-65. [PMID: 26998090].
6. Pepper MS, Mandriota SJ, Vassalli JD, Orci L, Montesano R. Angiogenesis regulating cytokines: activities and interactions. Curr Top Microbiol Immunol 1996; 213:31-67. [PMID: 9053296].
7. Xia XB, Xiong SQ, Xu HZ, Jiang J, Li Y. Suppression of retinal neovascularization by shRNA targeting HIF-1α. Curr Eye Res 2008; 33:892-902. [PMID: 18853324].
8. Lukiw WJ, Ottlecz A, Lambrou G, Grueninger M, Finley J, Thompson HW, Bazan NG. Coordinate activation of HIF-1 and NF-kappaB DNA binding and COX-2 and VEGF expression in retinal cells by hypoxia. Invest Ophthalmol Vis Sci 2003; 44:4163-70. [PMID: 14507857].
9. Watanabe D, Takagi H, Suzuma K, Suzuma I, Oh H, Ohashi H, Kemmochi S, Uemura A, Ojima T, Suganami E, Miyamoto N, Sato Y, Honda Y. Transcription factor Ets-1 mediates ischemia- and vascular endothelial growth factor-dependent retinal neovascularization. Am J Pathol 2004; 164:1827-35. [PMID: 15111329].
10. Zhang G, Fahmy RG, diGirolamo N, Khachigian LM. JUN siRNA regulates matrix metalloproteinase-2 expression, microvascular endothelial growth and retinal neovascularisation. J Cell Sci 2006; 119:3219-26. [PMID: 16847049].
11. Saint-Geniez M, Jiang A, Abend S, Liu L, Sweigard H, Connor KM, Arany Z. PGC-1a Regulates Normal and Pathological Angiogenesis in the Retina. Am J Pathol 2013; 182:255-65. [PMID: 23141926].
12. Wang M, Drucker DJ. The LIM domain homeobox gene isl-1: conservation of human, hamster, and rat complementary deoxyribonucleic acid sequences and expression in cell types of nonneuroendocrine lineage. Endocrinology 1994; 134:1416-22. [PMID: 7907017].
13. Pfaff SL. [1], Mendelsohn M, Stewart CL, Edlund T, Jessell TM. Requirement for LIM homeobox gene Isl1 in motor neuron generation reveals a motor neuron-dependent step in interneuron differentiation. Cell 1996; 84:309-20. [PMID: 8565076].
14. Bejarano-Escobar R, Álvarez-Hernán G, Morona R, González A, Martín-Partido G, Francisco-Morcillo J. Expression and function of the LIM-homeodomain transcription factor Islet-1 in the developing and mature vertebrate retina. Exp Eye Res 2015; 138:22-31. [PMID: 26122047].
15. Barzelay A, Ben-Shoshan J, Entin-Meer M, Maysel-Auslender S, Afek A, Barshack I, Keren G, George J. Potential role for islet-1 in post-natal angiogenesis and vasculogenesis. Thromb Haemost 2010; 103:188-97. [PMID: 20062933].
16. Liu J, Li W, Wang Y, Fan W, Li P, Lin W, Yang D, Fang R, Feng M, Hu C, Du Z, Wu G, Xiang AP. Islet-1 Overexpression in Human Mesenchymal Stem Cells Promotes Vascularization

Through Monocyte Chemoattractant Protein-3. Stem Cells 2014; 32:1843-54. [PMID: 24578274].

17. Barzelay A, Hochhauser E, Entin-Meer M, Chepurko Y, Birk E, Afek A, Barshack I, Pinhas L, Rivo Y, Ben-Shoshan J, Maysel-Auslender S, Keren G, George J. Islet-1 gene delivery improves myocardial performance after experimental infarction. Atherosclerosis 2012; 223:284-90. [PMID: 22727192].

18. Jiang J. [1], Xia XB, Xu HZ, Xiong Y, Song WT, Xiong SQ, Li Y. Inhibition of retinal neovascularization by gene transfer of small interfering RNA targeting HIF-1alpha and VEGF. J Cell Physiol 2009; 218:66-74. [PMID: 18767037].

19. Pérez de Lara MJ, Guzmán-Aránguez A, de la Villa P, Díaz-Hernández JI, Miras-Portugal MT, Pintor J. Increased levels of extracellular ATP in glaucomatous retinas: Possible role of the vesicular nucleotide transporter during the development of the pathology. Mol Vis 2015; 21:1060-70. [PMID: 26392744].

20. Smith LE, Wesolowski E, McLellan A, Kostyk SK, D'Amato R, Sullivan R, D'Amore PA. Oxygen-induced retinopathy in the mouse. Invest Ophthalmol Vis Sci 1994; 35:101-11. [PMID: 7507904].

21. Connor KM, Krah NM, Dennison RJ, Aderman CM, Chen J, Guerin KI, Sapieha P, Stahl A, Willett KL, Smith LE. Quantification of oxygen-induced retinopathy in the mouse: a model of vessel loss, vessel regrowth and pathological angiogenesis. Nat Protoc 2009; 4:1565-73. [PMID: 19816419].

22. Du A, Hunter CS, Murray J, Noble D, Cai CL, Evans SM, Stein R, May CL. Islet-1 is required for the maturation, proliferation, and survival of the endocrine pancreas. Diabetes 2009; 58:2059-69. [PMID: 19502415].

23. Hansel DE, Rahman A, Hidalgo M, Thuluvath PJ, Lillemoe KD, Shulick R, Ku JL, Park JG, Miyazaki K, Ashfaq R, Wistuba II, Varma R, Hawthorne L, Geradts J, Argani P, Maitra A. Identification of novel cellular targets in biliary tract cancers using 240 global gene expression technology. Am J Pathol 2003; 163:217-29. [PMID: 12819026].

24. Schmitt AM, Riniker F, Anlauf M, Schmid S, Soltermann A, Moch H, Heitz PU, Klöppel G, Komminoth P, Perren A. Islet 1 (Isl1) expression is a reliable marker for pancreatic endocrine tumors and their metastases. Am J Surg Pathol 2008; 32:420-5. [PMID: 18300808].

25. Rønneberg JA, Fleischer T, Solvang HK, Nordgard SH, Edvardsen H, Potapenko I, Nebdal D, Daviaud C, Gut I, Bukholm I, Naume B, Børresen-Dale AL, Tost J, Kristensen V. Methylation profiling with a panel of cancer related genes: 245 Association with estrogen receptor, TP53 mutation status and expression subtypes in sporadic breast cancer. Mol Oncol 2011; 5:61-76. [PMID: 21212030].

26. Hattori Y, Kanamoto N, Kawano K, Iwakura H, Sone M, Miura M, Yasoda A, Tamura N, Arai H, Akamizu T, Nakao K, Maitani Y. Molecular characterization of tumors from a transgenic mouse adrenal tumor model: comparison with human pheochromocytoma. Int J Oncol 2010; 37:695-705. [PMID: 20664939].

27. Dykxhoorn DM, Novina CD, Sharp PA. Killing the messenger:short RNAs that silence gene expression. Nat Rev Mol Cell Biol 2003; 4:457-67. [PMID: 12778125].

Articles are provided courtesy of Emory University and the Zhongshan Ophthalmic Center, Sun Yat-sen University, P.R. China. The print version of this article was created on 2 December 2016. This reflects all typographical corrections and errata to the article through that date. Details of any changes may be found in the online version of the article.